



## Article

# Modeling and Extended State Observer-Based Backstepping Control of Underwater Electro Hydrostatic Actuator with Pressure Compensator and External Load

Yong Nie <sup>1,2</sup>, Jiajia Liu <sup>2,3</sup> , Zhenhua Lao <sup>3</sup> and Zheng Chen <sup>1,2,3,\*</sup> 

<sup>1</sup> The State Key Laboratory of Fluid Power and Mechatronic Systems, Zhejiang University, Hangzhou 310027, China; ynie@zju.edu.cn

<sup>2</sup> Hainan Instruction of Zhejiang University, Sanya 572025, China; 12134019@zju.edu.cn

<sup>3</sup> Ocean College, Zhejiang University, Zhoushan 316021, China; 22034071@zju.edu.cn

\* Correspondence: zheng\_chen@zju.edu.cn; Tel.: +86-13505812510

**Abstract:** Electro hydrostatic actuator (EHA) has been successfully developed for flight control applications to replace the cumbersome centralized hydraulic system. It also has excellent potential for ocean applications due to its advantages on miniaturization and energy-savings. One of the special technologies for EHA's underwater application is pressure compensation, which is used to equalize the return pressure of the hydraulic system and the seawater pressure. This paper investigates the modeling and control design of underwater EHA to improve performance, especially considering the effect of additional pressure compensator and uncertain external load. The nonlinear hydraulic model is extended by the dynamic characteristics of the pressure compensator. Two low-order extended state observers were constructed to cope with the external load fore and the effect of the pressure compensator, respectively. The backstepping methods were designed to guarantee the robust stability of the entire high-order nonlinear hydraulic system. Finally, the theoretical proving and simulation on Matlab/Simulink are conducted to demonstrate the high tracking performance of the proposed control strategy.

**Keywords:** underwater electro hydrostatic actuator; extended state observer; compensator pressures; backstepping control



**Citation:** Nie, Y.; Liu, J.; Lao, Z.; Chen, Z. Modeling and Extended State Observer-Based Backstepping Control of Underwater Electro Hydrostatic Actuator with Pressure Compensator and External Load. *Electronics* **2022**, *11*, 1286. <https://doi.org/10.3390/electronics11081286>

Academic Editors: Luis Gomes, Weichao Sun and Weiyang Lin

Received: 21 March 2022

Accepted: 16 April 2022

Published: 18 April 2022

**Publisher's Note:** MDPI stays neutral with regard to jurisdictional claims in published maps and institutional affiliations.



**Copyright:** © 2022 by the authors. Licensee MDPI, Basel, Switzerland. This article is an open access article distributed under the terms and conditions of the Creative Commons Attribution (CC BY) license (<https://creativecommons.org/licenses/by/4.0/>).

## 1. Introduction

Electro hydrostatic actuator (EHA) is a direct-drive volume-controlled (pump-controlled) electro-hydraulic system. Compared with traditional valve-controlled hydraulic systems, EHA has the advantages of higher energy utilization efficiency, less throttling loss, and higher fault tolerance [1–3]. With the development of the marine and science of ocean, the demand for miniaturization and high-power equipment increases, which would expand the scope of practical applications for EHA. It can be used as a power unit in vehicle technology [4], underwater manipulator [5], and underwater cable cutting device. The underwater EHA adopted the pressure compensator technology so that the pressure of the oil return chamber is approximately equal to the pressure of seawater. Due to the changes of additional pressure compensator in the structure, the modeling and control need to be reconsidered.

EHA is a high-order (third-order) nonlinear system, and the challenge of EHA control lies in the complexity of the dynamic model. An equivalent transfer function model for EHA was established in [6–8], and the state-space model was adopted in most studies, such as [9,10]. Unfortunately, these studies do not consider pressure compensators and seawater forces. On the other hand, the mathematical modeling of the pressure compensator of the rolling diaphragm was carried out in [11,12]. The pressure compensator's pressure fluctuation characteristics were analyzed under different spring rates and areas of action using AMESim. However, the integrated modeling including an additional pressure

compensator for underwater EHA has not yet been established, and the corresponding control design has not yet been produced.

In the second place, to achieve high control accuracy of EHA, the high-order-dynamic, inherent nonlinear characteristic, and uncertainties (including parameter uncertainties, structured uncertainties, and unstructured uncertainties) need to be coped with. Nowadays, numerous advanced control methods have been developed, like backstepping control [13], adaptive control [14], adaptive robust control [15–17], sliding mode control [18,19], and disturbance-based control [20,21]. Specifically, adaptive backstepping control is proposed for EHA with parametric uncertainties [22] but hardly handles unstructured uncertainties. Adaptive robust control (ARC) [16] was proposed to deal with structured and unstructured uncertainties for the hydraulic system. However, it needs high gain to eliminate the bounded uncertainties and ask for complex calculations and larger known information. These approaches adopt feedback control rather than feedforward compensation control. Disturbance-based control (DOB) methods are another frame to solve the unstructured uncertain, inherent nonlinear characteristic. For example, active disturbance rejection control (ADRC) can overcome large unstructured uncertainties with less information by using an extended state observer (ESO) to estimate generalized disturbances and compensate them feedforward. Nevertheless, the perfect performance quite depends on the observer gain, where the higher the order dynamic is, the higher gain is needed. However, in practice, the high gain will usually cause the observer's oscillation due to actual effects. In order to avoid the use of higher gain, the integration methods combining observe technology, robust control, and adaptive control were carried out [23] and verified in DC motor control [24] and hydraulic system [25], in which ESO is used to observe the structured uncertainties, robust control is used to deal with the observer error, inherent nonlinear characteristic, and unstructured uncertainties, and adaptive methods are used to cope with the parameter uncertainties. It is a powerful tool for EHA systems. However, many parameters need to be designed, especially the adaptive law, which may not play an important role, and ESO in [25] does not estimate the unstructured uncertainties. The order of ESO is high due to the high hydraulic system; hence, adding the hardware sensor to directly obtain and indirectly calculate the states to reduce the order of ESO and estimate the unstructured uncertainties is necessary and feasible.

In addition, in order to reduce the energy consumption, the dual variable control is proposed in [26], and pump and valve combined control is adopted in [27–29]. The accurate model considered nonlinear actuator friction and the nonlinear pump flow rate at the low pump speeds is further established in [30–32] to improve low-speed control performance. Furthermore, the existing control methods on EHA show that position tracking is usually achieved at a millimeter-level. The experimental result [33] remains at 0.1 mm using quantitative feedback theory. From [31], the ARC controller's tracking error is within 2 mm. The PID controller's position control accuracy is 20 mm [34]. Herein, nearly all these results are limited to the conventional EHA systems, and the control for underwater EHA has not been carried out.

This article establishes the underwater electro hydrostatic actuator model, including the sea pressure compensator, and proposes an extended state observer-based backstepping control method. The principal value and contributions of this study are summarized as follows

- A new underwater electro hydrostatic actuator model with the pressure compensator. If the sensors can measure the pressure compensator state, the disturbance of the compensator could be compensated based on the model; otherwise, it is observed by extending the state observer.
- The backstepping controller combined two low-order extended state observers for the underwater EHA system. The uncertain external load and the disturbance effect caused by the pressure compensator are estimated and then compensated by feedforward. Combining the backstepping method leads to transient motion tracking and final tracking performance.

The rest of the parts of this paper are illustrated as follows: Section 2 gives the modeling and formulation, Section 3 demonstrates the extended state observer-based backstepping control design, and Section 4 shows the influence of the pressure compensator and the advantage of the proposed control strategy.

## 2. Materials and Methods

### 2.1. Modeling and Problem Formulation

#### 2.1.1. System Description

In addition to conventional parts such as an electric motor, a hydraulic pump, a new valve opened by differential pressure, and a hydraulic cylinder within a closed-loop circuit, the underwater EHA also has pressure compensators. As shown in Figure 1, our underwater prototype EHA uses an electric servo-motor, micro piston pump, signal rod cylinder, and rolling diaphragm pressure compensator. The rolling diaphragm pressure compensator is used to overcome seawater pressure and compensates for the differential flow of the cylinder ports in both extension and retraction cases. The pressure control valve decides the charging and discharging process of the compensator. The hydraulic schematic diagram is shown in Figure 2. After the electric motor starts to rotate, the pump unit delivers the flow while filling the chamber. Then the oil builds up the chamber pressure and controls the displacement of the hydraulic actuator. Due to the asymmetrical cylinder, the pressure compensator compensates for the different flows. The compensated flows inject the compensator in retraction. On the contrary, the flow flows. In addition, the position and velocity sensor of the piston rod and the pressure sensors are installed.

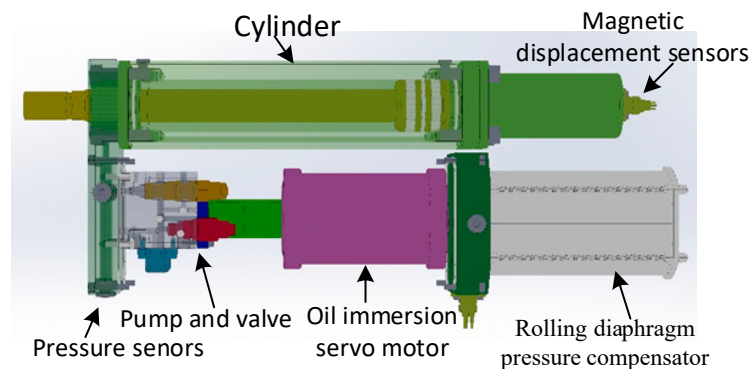


**Figure 1.** Structural design of underwater EHA: An electric servo-motor, micro piston pump, signal rod cylinder, and rolling diaphragm pressure compensator. The addition of a rolling diaphragm pressure compensator is used to overcome seawater pressure.

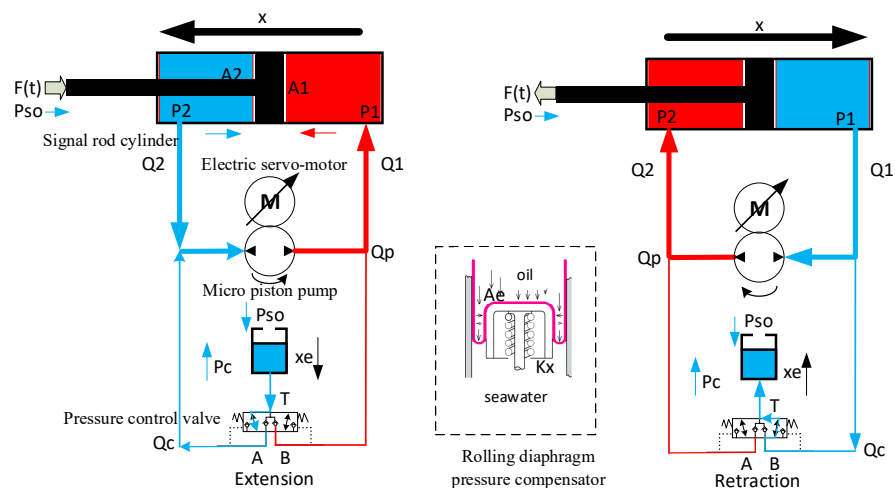


**Figure 2.** Hydraulic schematic diagram for EHA extension and retraction with pressure compensator.

### 2.1.2. Modeling of the Underwater EHA

This section is concerned with modeling the underwater EHA, including the sea pressure compensator. The mathematical model of EHA includes the dynamic of the cylinder described by the second Newton’s Law, and the system’s flow rate is derived from the EHA system’s configuration.

#### 1. Dynamic of cylinder

The dynamics of a cylinder can be modeled as

$$m_L \ddot{x}_L = (P_1 - P_{s0})A_1 - (P_2 - P_{s0})A_2 - B_m \dot{x}_L - F(t) \tag{1}$$

where  $x_L$  and  $m_L$  represent the actual position and the inertia of the load.  $B_m$  is the viscous friction coefficient.  $P_1, P_2, P_{s0}$  represent the pressures of the head, rod, and the sea environment.  $F(t)$  is denoted by the uncertain external load force, including the seawater disturbance force.  $A_1, A_2$  represent the area on each side of the cylinder piston.

The pressure dynamic of the two chambers can be described as

$$\begin{aligned} \frac{V_1}{\beta_e} \dot{P}_1 &= -A_1 \dot{x}_L + Q_1 + L_1 \\ \frac{V_2}{\beta_e} \dot{P}_2 &= A_2 \dot{x}_L - Q_2 + L_2 \end{aligned} \tag{2}$$

where  $V_1 = V_{01} + A_1 x_L, V_2 = V_{02} - A_2 x_L$  represent the total hydraulic compressible volumes when the position is  $x_L$ .  $Q_1, Q_2$  are the flow of the two chambers and will be defined later.  $L_1, L_2$  are the total leakage of the  $P_1, P_2$  chambers, respectively.

#### 2. Flows rate with the pressure compensator

Based on the working principles discussed earlier, the pressure compensator compensates for the difference flows caused by the asymmetric. The flows satisfy the following equations, respectively.

When the piston rod extends, the flows equations are written as

$$\begin{aligned} Q_1 &= Q_p \\ Q_2 &= Q_p - Q_c \end{aligned} \tag{3}$$

On the contrary, the flows equation is written as

$$\begin{aligned} Q_1 &= Q_c + Q_p \\ Q_2 &= Q_p \end{aligned} \tag{4}$$

where  $Q_p$  is the pump flow rate and satisfied  $Q_p = D_p \cdot w - L_p$ .  $Q_c$  is the different flows of the pressure compensator and satisfied  $Q_c = A_e \dot{x}_c - \frac{V_c}{\beta_e} \dot{P}_c$ .  $D_p$  is the pump flow coefficient.  $w$  is the servo-motor speed.  $L_p$  is the total leakage of the pump.

#### 3. Simple dynamic of the pressure compensator

The pressure dynamic of the chamber of the pressure compensator can be described as

$$Q_c = A_e \dot{x}_c - \frac{V_c}{\beta_e} \dot{P}_c$$

where  $V_c$  represent the hydraulic compressible volumes when the diaphragm-piston is  $x_c$ .  $P_c$  is the pressure of the compensator.  $A_e$  is the effective area of the rolling diaphragm as shown in Figure 2.  $K_x$  is the spring stiffness.  $x_c$  is the placement of the diaphragm-piston assembly.

Thanks to the fact that  $P_c A_e = P_{s0} A_e + K_x x_c$  which follows from reference [12] in the static state,  $\dot{P}_c$  can be written as  $\dot{P}_c = \frac{K_x \dot{x}_c}{A_e}$ . Therefore,  $Q_c$  can be described as

$$Q_c = A_e \dot{x}_c - \frac{V_c}{\beta_e} \left( \frac{K_x \dot{x}_c}{A_e} \right). \tag{5}$$

### 2.1.3. Problem Formulation

Combining Equations (1)–(4), and the pressure compensator flows Equation (5), the state variables are defined as  $[x_1, x_2, x_3] = [x_L, \dot{x}_L, (P_1 - P_{s0})A_1 - (P_2 - P_{s0})A_2]$ . Thus, the entire system can be expressed as follows in the case of extension.

$$\begin{aligned} \dot{x}_1 &= x_2 \\ \dot{x}_2 &= \frac{1}{m_L} x_3 - \frac{B_m}{m_L} x_2 - \frac{F(t)}{m_L} \\ \dot{x}_3 &= -\alpha(t, x_1) x_2 + \beta(t, x_1) (D_p \cdot w) - \gamma(t, x_1, x_c, \dot{x}_c) + \varphi(x_1, L_1, L_2, L_p) \end{aligned} \tag{6}$$

where  $\alpha(t, x_1) = \frac{\beta_e A_1 A_1}{V_1} + \frac{\beta_e A_2 A_2}{V_2}$ ,  $\beta(t, x_1) = \frac{\beta_e A_1}{V_1} + \frac{\beta_e A_2}{V_2}$  are the nonlinear and time-varying term.  $\gamma(t, x_1, x_c, \dot{x}_c)$  the disturbance of additional pressure compensator and is depicted by  $\gamma(t, x_1, x_c, \dot{x}_c) = \begin{cases} \frac{\beta_e A_2 A_e}{V_2} - \frac{V_c A_2 K_x}{V_2 A_e} & \dot{x}_L \geq 0 \\ -\left(\frac{\beta_e A_1 A_e}{V_1} - \frac{V_c A_1 K_x}{V_1 A_e}\right) & \dot{x}_L < 0 \end{cases}$ .  $\varphi(x_1, L_1, L_2, L_p) = L_1 \left(\frac{\beta_e A_1}{V_1}\right) - L_2 \left(\frac{\beta_e A_2}{V_2}\right) - L_p \left(\frac{\beta_e A_1}{V_1} + \frac{\beta_e A_2}{V_2}\right)$  the total leakage.

The leakage coefficients  $L_1, L_2, L_p$  belong to  $[0, 2.4 \times 10^{-11}]$  referring to [35] and  $\frac{\beta_e A_1}{V_1}, \frac{\beta_e A_2}{V_2}$  lie in the interval  $[2 \times 10^9, 14 \times 10^9]$  according to model parameters. Thus, the value of  $\varphi(x_1, L_1, L_2, L_p)$  varies around 10. However, the disturbance of the additional pressure compensator  $\gamma(t, x_1, x_c, \dot{x}_c)$  is about 10 to the 4th power, which will be verified later. Therefore, the disturbance can be regarded as the main effect compared with leakage for the underwater EHA.

The task is to achieve high accuracy position control. We adopt the observer to estimate the disturbances  $\gamma(t, x_1, x_c, \dot{x}_c)$  caused by the pressure compensator and the uncertain external load  $F(t)$ . Then these uncertainties are eliminated by feedforward compensation. Meanwhile, the backstepping strategy is designed for the cylinder actuator motion tracking to deal with the high-order dynamics and high nonlinearities of the entire underwater electro-hydraulic system.

## 2.2. Backstepping Control Design with Extended State Observer

### 2.2.1. Extend State Observer Design

This section designed two low-order extend states observers to observe the unknown external load  $F(t)$  and the disturbance  $\gamma(t, x_1, x_c, \dot{x}_c)$ . The position and velocity sensor measure the system states  $x_1$  and  $x_2$ . Meanwhile,  $x_3$  can be obtained by  $P_1$  and  $P_2$  pressure sensor. Consequently, the order of extended states observers (ESO) can be reduced. Define  $x_4 = F(t)/m$  and the disturbance  $x_5 = \gamma(t, x_1, x_c, \dot{x}_c)$ .  $g_1(t), g_2(t)$  as the time derivative of  $x_4, x_5$ . Thus, the extended system model can be rearranged as

$$\begin{aligned} \dot{x}_1 &= x_2 \\ \dot{x}_2 &= \frac{1}{m_L} x_3 - \frac{B_m}{m_L} x_2 - x_4 \\ \dot{x}_3 &= -\alpha(t, x_1) x_2 + \beta(t, x_1) (D_p \cdot w) - x_5 \\ \dot{x}_4 &= g_1(t) \\ \dot{x}_5 &= g_2(t) \end{aligned} \tag{7}$$

where  $g_1(t) = \frac{\dot{F}(t)}{m_L}, g_2(t) = \dot{\gamma}(t, x_1, x_c, \dot{x}_c)$ .

**Assumption 1.** According to the actual physics system, we assume  $|g_1(t)| \leq M_1, \|g_2(t)\| \leq M_2$  where  $M_1$  and  $M_2$  are unknown. The  $\gamma(t, x_1, x_c, \dot{x}_c)$  is bound due to the state  $x_1$  and  $x_c$  are bound.  $\dot{F}(t)$  is the change rate of uncertain external load force and bounded.

Based on the extended system model, the linear extended state observers (LESO) are then constructed as

$$\begin{aligned} \dot{\hat{x}}_2 &= R_1(x_1, x_2, t, u) - \hat{x}_4 + \alpha_1 \frac{(y_2 - \hat{x}_2)}{\varepsilon_1} \\ \dot{\hat{x}}_4 &= \alpha_2 \frac{(y_2 - \hat{x}_2)}{\varepsilon_1^2} \end{aligned} \tag{8}$$

$$\begin{aligned} \dot{\hat{x}}_3 &= R_2(x_1, x_2, t, u) - \hat{x}_5 + \alpha_1 \frac{(y_3 - \hat{x}_3)}{\varepsilon_1} \\ \dot{\hat{x}}_5 &= \alpha_2 \frac{(y_3 - \hat{x}_3)}{\varepsilon_1^2} \end{aligned} \tag{9}$$

where  $\hat{x}_2, \hat{x}_3, \hat{x}_4,$  and  $\hat{x}_5$  are the estimate of the  $x_2, x_3, x_4,$  and  $x_5$ , the  $y_1, y_2, y_3$  are the measured value of the  $x_1, x_2, x_3$ . The same gain  $\alpha_1, \alpha_2$  is designed for two observers and  $\varepsilon_1 > 0$  is a small constant, which can be designed.  $R_1(x_1, x_2, t, u) = \frac{1}{m_L} [(P_1 - P_{s0})A_1 - (P_2 - P_{s0})A_2] - \frac{B_m}{m_L} x_2, R_2(x_1, x_2, t, u) = -\alpha(t, x_1)x_2 + \beta(t, x_1)D_p u$  can be calculated using the information of  $y_1, y_2, y_3, P_1, P_2$ .

The dynamic of the state estimation errors can be written as the vector

$$\dot{\hat{\mathbf{e}}}(t) = \mathbf{A}\hat{\mathbf{e}}(t) + \mathbf{B}\mathbf{M}(t) \tag{10}$$

where  $\hat{\mathbf{e}} = [\hat{e}_2, \hat{e}_4, \hat{e}_3, \hat{e}_5]$ ,  $\hat{e}_2 = y_2 - \hat{x}_2, \hat{e}_3 = y_3 - \hat{x}_3, \hat{e}_4 = x_4 - \hat{x}_4, \hat{e}_5 = x_5 - \hat{x}_5$  and  $\mathbf{A} = \begin{bmatrix} A_1 & 0 \\ 0 & A_1 \end{bmatrix}, \mathbf{B} = \begin{bmatrix} B_1 \\ B_1 \end{bmatrix}, A_1 = \begin{bmatrix} -\frac{\alpha_1}{\varepsilon} & 1 \\ -\frac{\alpha_2}{\varepsilon^2} & 0 \end{bmatrix}, B_1 = \begin{bmatrix} 0 \\ 1 \end{bmatrix}, \mathbf{M}(t) = [0 \quad g_1(t) \quad 0 \quad g_2(t)]$ .

**Theorem 1.** *The observer’s errors asymptotically converge to  $\hat{e}_4(\infty) = \frac{\alpha_1 \varepsilon_1}{\alpha_2} M_1 \hat{e}_5(\infty) = \frac{\alpha_1 \varepsilon_1}{\alpha_2} M_2$ , while  $t \rightarrow \infty$ . The rate of convergence depends on the parameters of  $\alpha_1, \alpha_2, \varepsilon_1$ , and the transient error is bounded in the transient progress, which will be eliminated later by using a robust control function at each step of the design to achieve a guaranteed final tracking accuracy.*

**Proof of Theorem 1.** The solution of the system (10) can be written as  $\varepsilon_x = \varepsilon_s + \varepsilon_u$ , where  $\varepsilon_s$  is the zero-input response satisfying  $\dot{\varepsilon}_s = \mathbf{A}\varepsilon_s$ , and  $\varepsilon_u = \int_0^t \hat{\mathbf{e}}^{\mathbf{A}(t-\tau)} \mathbf{B}\mathbf{M}(\tau) d\tau; t \geq 0$  is the zero-state response. Noting assumption 1 and the fact that the matrix  $\mathbf{A}$  is stable, one has

$$\varepsilon_u \in \Omega_\varepsilon \triangleq \{\varepsilon_u : |\varepsilon_u(t)| \leq \delta_u\}$$

where  $\delta_u$  is unknown.

Furthermore, when  $t \rightarrow \infty$

$$\begin{aligned} \|\hat{\mathbf{e}}(t)\| &\leq \hat{\mathbf{e}}^{\mathbf{A}t} \|\hat{\mathbf{e}}(0)\| + \int_0^t \hat{\mathbf{e}}^{\mathbf{A}(t-\tau)} \mathbf{B}\mathbf{M}(\tau) d\tau \\ \|\hat{\mathbf{e}}(\infty)\| &\leq \|\mathbf{A}^{-1}(I - \hat{\mathbf{e}}^{\mathbf{A}t})\mathbf{B}\| \|\mathbf{M}(t)\| \end{aligned} \tag{11}$$

The first item of the Formula (11) will converge to zero, and the second item expressing the observer errors  $\hat{e}_4, \hat{e}_5$  asymptotically converges to  $\hat{e}_4(\infty) = \frac{\alpha_1 \varepsilon_1}{\alpha_2} M_1 \hat{e}_5(\infty) = \frac{\alpha_1 \varepsilon_1}{\alpha_2} M_2$ . □

### 2.2.2. Backstepping Controller Design

In order to deal with the high order dynamics and the nonlinearities of the hydraulic system, the robust backstepping strategy is designed based on the observer value  $x_4, x_5$ .

The position tracking error is defined as  $z_1 = x_1 - x_{1d}$  and  $z_2$  is defined as

$$z_2 = \dot{z}_1 + k_1 z_1 = x_2 - x_{2d}, \quad x_{2d} = \dot{x}_{1d} - k_1 z_1 \tag{12}$$

where  $x_{1d}$  represents the desired trajectory and  $k_1$  is the positive feedback gain. Obviously, it holds that from reference [31]. Making converge to zero is equivalent to making  $z_1$  converge to zero. Hence, the rest aims at minimizing  $z_2$ .

Step 1:

The error dynamics is written as

$$\dot{z}_2 = \frac{1}{m_L} x_3 - \frac{B_m}{m_L} x_2 - \Delta d_1(t) - \dot{x}_{2d} \tag{13}$$

where  $\Delta d_1(t) = \frac{F(t)}{m_L} - \hat{x}_4$ , it is the observer error for the external load.

We defined  $F_{Ld}$  as the desired value of  $x_3$  and the virtual control input for Step 1, so the control law can be written as

$$\begin{aligned} F_{Ld} &= F_{Ld1} + F_{Ld2} \\ F_{Ld1} &= B_m x_2 + m_L \dot{x}_{2eq} - k_2 z_2 \\ F_{Ld2} &= -\frac{z_2}{4\varepsilon_2} \end{aligned} \tag{14}$$

where  $F_{Ld1}$  is a physical model-based compensation term and a backstepping-based stabilizing feedback term,  $k_2$  is the feedback gain.  $F_{Ld2}$  is the robust feedback term and is chosen to satisfy the following robust conditions.

$$\begin{aligned} z_2(F_{Ld2} + \Delta d_1) &\leq \varepsilon_2 \\ z_2 F_{Ld2} &\leq 0 \end{aligned} \tag{15}$$

where  $\varepsilon_2 > 0$  can be arbitrarily small.

Step 2:

We define  $z_3 = F_L - F_{Ld}$  as the error of Step2. Let the  $w$  as the control input of Step 2 to make  $z_3$  converge to zero or a small value.

The error dynamic of  $z_3$  when the cylinder piston extends can be written as

$$\dot{z}_3 = \dot{x}_3 - \dot{F}_{LD} = -\alpha(t, x_1)x_2 + \beta(t, x_1)(D_p \cdot w) - \Delta d_2 - \dot{F}_{Ld} \tag{16}$$

where  $\dot{F}_{Ld} = \frac{\partial F_{Ld}}{\partial x_1} x_2 + \frac{\partial F_{Ld}}{\partial x_2} \dot{x}_2 + \frac{\partial F_{Ld}}{\partial t}$  will be calculated by the  $x_1, x_2, P_1, P_2$ .  $\Delta d_2 = x_4 - \hat{x}_4$  is observer error, which will be covered by roust feedback.

The control input  $w$  is designed as

$$\begin{aligned} w_d &= w_{d1} + w_{d2} \\ w_{d1} &= \frac{1}{\beta(t, x_L)D_p} x_2 + \frac{1}{\beta(t, x_L)D_p} \dot{F}_{Ld} - \frac{1}{\beta(t, x_L)D_p} k_3 z_3 \\ w_{d2} &= -\frac{1}{\beta(t, x_L)D_p} \left( \frac{z_3}{4\varepsilon_3} \right) \end{aligned} \tag{17}$$

where  $w_{d1}$  is a physical model-based compensation term and a backstepping-based stabilizing feedback term,  $k_3$  is the feedback gain,  $w_{d2}$  is the robust feedback term and is chosen to satisfy the following robust conditions.

$$\begin{aligned} z_3(w_{d2} + \Delta d_2) &\leq \varepsilon_3 \\ z_3 w_{d2} &\leq 0 \end{aligned} \tag{18}$$

where  $\varepsilon_3 > 0$  can be arbitrarily small.

**Theorem 2.** A positive definite function is defined as  $V_3 = \frac{1}{2}z_1 \cdot z_1 + \frac{1}{2}z_2 \cdot z_2 + \frac{1}{2}z_3 \cdot z_3$ . Considering the backstepping control law with the observer compensation, the transient performance is quantified by

$$V_3 \leq \exp(-2\lambda t)V_3(0) + \frac{\varepsilon}{2\lambda}[1 - \exp(-2\lambda t)] \tag{19}$$

where  $\lambda = \min\left\{k_1, \frac{B_m}{m_L} + k_2, k_3\right\}$ ,  $\varepsilon = \varepsilon_2 + \varepsilon_3$  in which  $\varepsilon_2$  and  $\varepsilon_3$  are robust parameters given, respectively.

**Proof of Theorem 2.**

$$\begin{aligned} \dot{V}_3 &= -k_1 z_1^2 - \left(\frac{B_m}{m_L} + k_2\right) z_2^2 - k_3 z_3^2 + z_2(F_{Ld2} + \Delta d) + z_3(w_{d2} + \Delta d_2) \\ &\leq -k_1 z_1^2 - \left(\frac{B_m}{m_L} + k_2\right) z_2^2 - k_3 z_3^2 + \varepsilon_2 + \varepsilon_3 \\ &\leq -2\lambda V_3 + \varepsilon \end{aligned} \tag{20}$$

□

**Remark 1.** The proposed disturbance-observer-based backstepping controller not only estimates the disturbance caused by the pressure compensator and the uncertain external load but also guarantees the transient performance with the bounded tracking error. The transient tracking error and the final tracking error can be improved by increasing the robust feedback gains  $\lambda$ . What is more, we can avoid the high gain feedback to limit the final error by adjusting the observer gain  $\alpha_1, \alpha_2, \varepsilon_1$ .

**3. Results**

*3.1. Simulation Setup*

In order to verify the performance of the proposed extended state observer-based backstepping controller, the simulation was carried out in Simulink/Matlab. The parameters of the simulation system are designed in Table 1. The step of calculating simulation set 0.001 s, and chose the fixed step, which is consistent with the actual control physics. We established the mathematical model by the S-function according to (6); the variable’s value can be directly obtained and calculated indirectly from S-function. The extended state observer and backstepping controller were designed according to (11) and (19).

**Table 1.** Parameter of the simulation.

Parameter	Value	Parameter	Value
$m_L$	100 kg	$\beta_e$	$7 \times 10^8$
$B_m$	2000 N/(m/s)	$P_{s0}$	$4.5 \times 10^6$ Pa
$A_1$	$2.3758 \times 10^{-3}$ m <sup>2</sup>	$V_{c0}$	0.0716 m <sup>3</sup>
$A_2$	$1.76 \times 10^{-3}$ m <sup>2</sup>	$K_x$	3.1 N/mm
$A_e$	$14.314 \times 10^{-3}$ m <sup>2</sup>	$L_{1,2,p}$	$[0, 2.4 \times 10^{-11}]$

Given that the actual system is different from the simulation model, the parameters  $\beta_e, B_m$  are designed differently in the simulation model and controller.

- (1) In the simulation model:  $\beta_e = 7 \times 10^8, B_m = 2000$  N/(m/s).
- (2) In controller and observer:  $\beta_e = 0.95 \times 7 \times 10^8, B_m = 0.95 \times 2000$  N/(m/s).

In addition, we design two terms  $\Delta \tilde{d}_1, \Delta \tilde{d}_2$  which simulate the difference between the actual model and the simulation model.  $\Delta \tilde{d}_1$  is chosen in the sinusoidal form in consideration of the wave’s fluctuating nature.  $\Delta \tilde{d}_2$  is selected as an exponential form of dissipation. In fact, they will be observed and compensated by extended stated observers.

$$\begin{aligned} \Delta \tilde{d}_1 &= 20 \times \sin(1 \times (t - 1)) \\ \Delta \tilde{d}_2 &= (100 + 1000 \times \exp(-0.1 \times (t - 1))) \times \sin(1 \times t) \end{aligned}$$

We make use of two control methods. The result demonstrates the effectiveness of the proposed backstepping controller with extended state observer and illustrates the disturbance of the pressure compensator.

- (1) C1: Backstepping controller with an extending state observer.
- (2) C2: The classic backstepping controller.
- (3) C4: The contractional PID controller.
- (4) C5: The ADRC (active disturbance rejection control) controller.



The desired tracking trajectory is designed as a continuous and smooth point–point curve, existing higher derivative, as shown in Figure 3. The uncertain external load  $F(t) = \begin{cases} 200 \times (1 - e^{-0.1(t-1)^3}), t < 15 \\ 200 \times (1 - e^{-0.1(t-15)^3}), 15 \leq t < 30 \end{cases}$ . The controller parameters are as follows:  $\alpha_1 = 10.8, \alpha_2 = 20.8, \varepsilon_1 = 0.005, k_1 = 30, k_2 = 80, k_3 = 200, \varepsilon_2 = 0.001, \varepsilon_3 = 0.001$  for C1-High gain,  $k_1 = 6, k_2 = 16, k_3 = 40$  for C1-Low gain;  $k_1 = 30, k_2 = 80, k_3 = 200$  for C2.  $k_p = 10000, k_i = 100$  for C4.  $\delta = 0.5, h = 0.1$  for C5 [35].

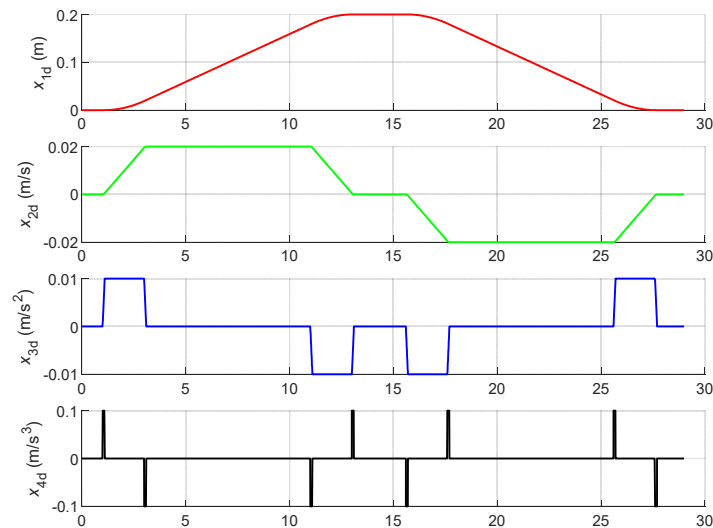


**Figure 3.** Desired tracking trajectory of EHA completion of an extension and retract.

### 3.2. Comparative Results

Figure 4 represents the tracking errors of C1, C2, C4, and C5. The errors are in the degree of a millimeter for both controllers. The error of C1 is smaller than the others. That is to say, the disturbance and uncertainties decrease the accuracy of position control, which means compensation for these is essential. The tracking error of C2 caused by the disturbance and uncertainty is also increasing for the most progress. The PID controller needs a large gain, and the performance is hard to improve further. The ADRC controller is the same as the PID, but it adopted the nonlinear PID and consisted of the ESO so that it can achieve better accuracy. Still, the final tracking accuracy is not very pleased. However, the C1 with extended state observer is favorable in two aspects. On the one hand, it can eliminate the transient error depending on the observed performance. On the other hand, it can reduce the tracking error further with the gain parameter increasing; the final tracking accuracy can be achieved at a higher level. As to the gain parameter, the C1 controller reduces the high gain parameters and can obtain a higher accuracy at the same gain value.

As shown in Figure 5, the output of the C1 controller varies less, and it is suitable for the service life of motor components and compensators. In the meantime, the proposed controller has a better ability to overcome transient disturbance. When a shock disturbance  $\Delta \tilde{d}_2$  is given at 20 s, the control input of the C1 controller can converge quickly because of the compensation of the extended state observer. Still, the control output of the C2 controller fluctuates wildly.

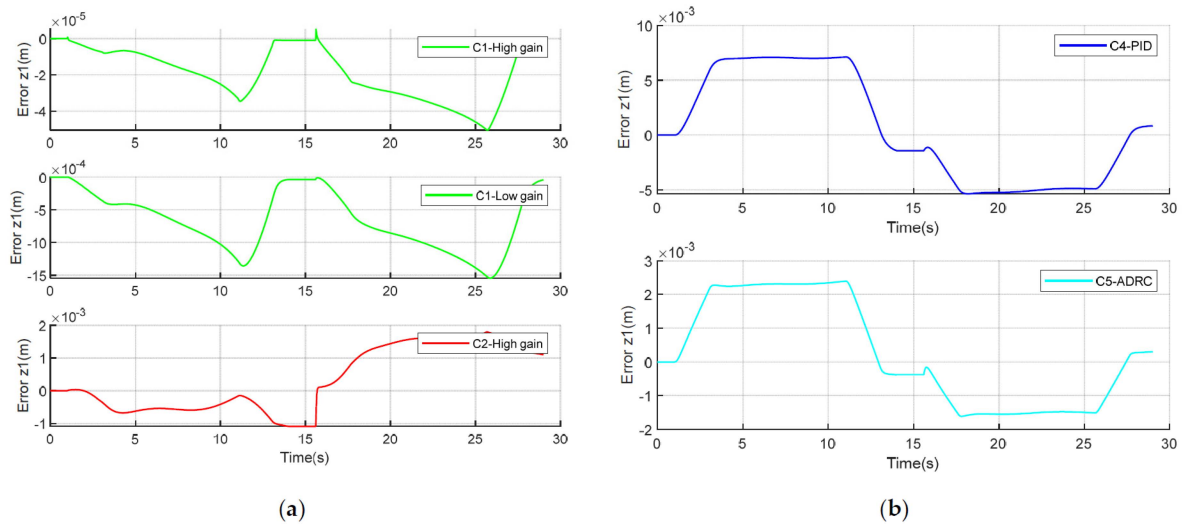


Figure 4. Tracking error. (a) C1–High gain, C1–Low gain, and C2–High gain. (b) C4–PID, C5–ADRC.

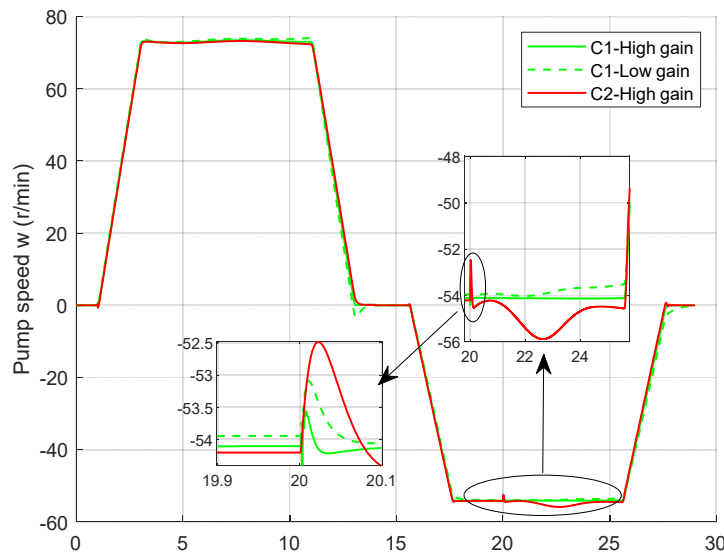


Figure 5. Pump speeds for C1 and C2 and response to the shock disturbance.

The errors  $\hat{e}_4, \hat{e}_5$  are depicted in Figure 6, which shows that the observer errors are bounded, in which uncertain load error is about  $5 \times 10^{-3}$  N (0.25%FS), and disturbance error of pressure compensator is approximately 300 (N·m)/s (0.3%FS). The result shows that the observer can achieve high observer performance. The disturbance effect increases with the piston rod approaching the left endpoint in an extended case. Because when the piston rod is extended,  $V_2$  is significantly decreasing, the  $\dot{x}_e$  varies little, as shown in Figures 7 and 8. Herein, it leads to an increase of the disturbance of the pressure compensator according to (6). The maximum influence of the rolling diaphragm pressure compensator happens at the end of the actuator.

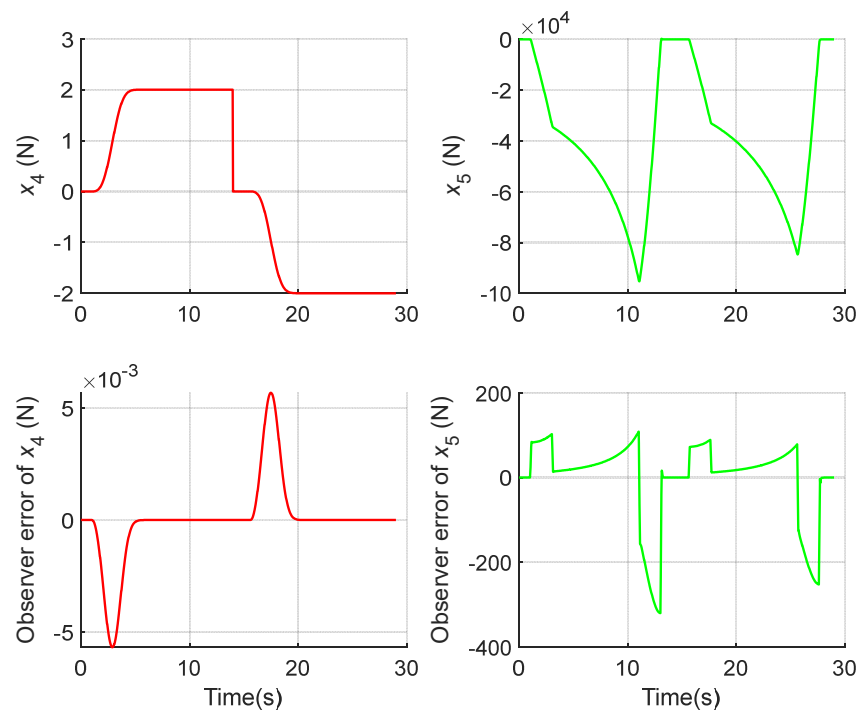


Figure 6. The external load  $x_4$ , compensator disturbance  $x_5$ , and their errors  $\hat{e}_4, \hat{e}_5$  for observer.

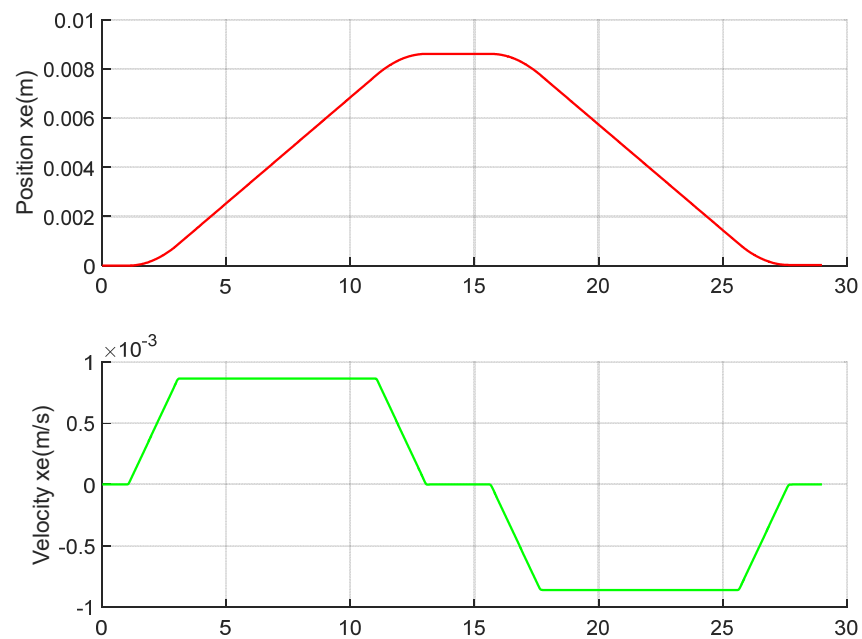
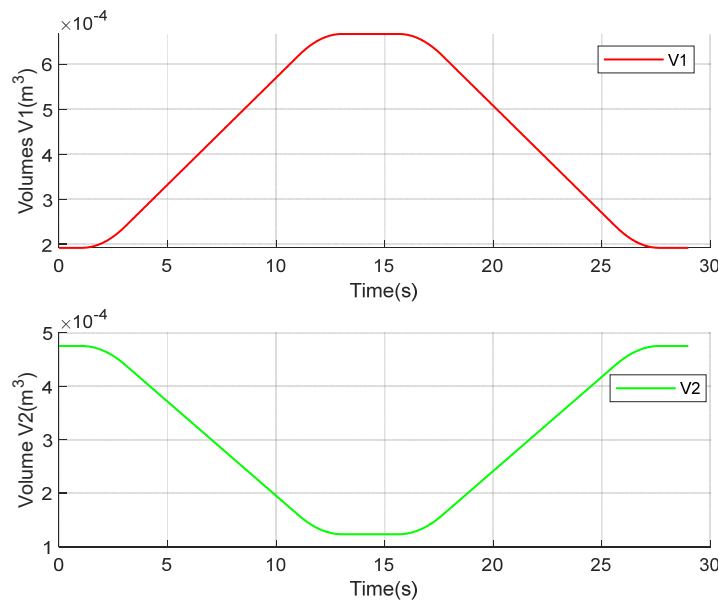


Figure 7. The position and velocity of the rolling diaphragm.



**Figure 8.** Volume changes of V1 and V2 in one period of motion.

Compared with the tracking performances of C1 and C2 quantitatively, the numerical errors [27] of the motion tracking results are listed in Table 2, where  $\|e\|_{\max}(m)$  is the maximum value of tracking error  $z_1$ ,  $\|e\|_1(m \cdot s) = \int_{t_0}^{t_f} \|z_1(t)\| dt$  and  $\|e\|_s(m)$  is the final errors. It clearly holds that C1 achieved higher tracking accuracy than C2, C4, and C5. The proposed controller not only achieves a prescribed tracking transient performance but also guarantees final tracking accuracy and the high gain feedback is also avoided by the extended state observer.

**Table 2.** Numerical comparison of tracking errors.

Controllers	$\ e\ _{\max}(m)$	$\ e\ _1(m \cdot s)$	$\ e\ _s(m)$
C1 high gain	$5 \times 10^{-5}$	0.538	$9.5 \times 10^{-7}$
C1 low gain	$1.5 \times 10^{-3}$	19.172	$3.5 \times 10^{-5}$
C2 high gain	$1.8 \times 10^{-3}$	25.164	0.001
C4 PID	$7.1 \times 10^{-3}$	125	$8.2 \times 10^{-4}$
C5 ADRC [35]	$2.4 \times 10^{-3}$	39.54	$3 \times 10^{-4}$

#### 4. Discussion

Prior works focusing on the conventional EHA have achieved the errors limited to 2 mm, such as ARC controller [32], and quantitative feedback controller [34]. Our research limited the position errors to 0.05 mm by the simulation for the underwater EHA system. Compared with the PID controller [8], the control performance shows pronounced improvement. We found that the effect of additional pressures compensator and external load decreases the position control performance, so we designed the extended state to estimate these and used the feedforward method to compensate. To the best of our knowledge, this is the first study to investigate the modeling and control of underwater EHA. The proposed control method ensures the position control performance, and it can overcome the influence of the pressure compensator and external load. However, some limitations are worth noting. Although the theory and simulation supported our results, the actual experiment should verify further.

## 5. Conclusions

In this paper, a modeling and backstepping controller with an extended state observer is proposed for an underwater electro hydrostatic actuator system. Firstly, the model of underwater EHA is established and analyzed with a pressure compensator. Secondly, two low extended state observers are designed to handle the unmeasured state and uncertain external load, which are solved by feed-forward compensation. In addition, the backstepping controller guarantees the stability of the entire high order nonlinear hydraulic system. Finally, the high tracking performance of the controller is proved by the Simulink/Matlab based on an underwater electro hydrostatic system model.

**Author Contributions:** Conceptualization, Z.C. and Y.N.; methodology, J.L. and Z.C.; software, J.L.; validation, Y.N., Z.C., Z.L. and J.L.; formal analysis, J.L.; investigation, Z.L.; resources, Y.N.; data curation, Z.L.; writing—original draft preparation, J.L.; writing—review and editing, J.L. and Z.C.; project administration, Y.N.; funding acquisition, Y.N. All authors have read and agreed to the published version of the manuscript.

**Funding:** This work is supported by Hainan Provincial National Natural Science Foundation of China (No. 521MS065), the Hainan Special PhD Scientific Research Foundation of Sanya Yazhou Bay Science and Technology City (No. HSPHDSRF-2022-04-004), and National Natural Science Foundation of China (No. 51875508).

**Acknowledgments:** We wish to thank Qimeng Guo and Xinran Wu for their advices on prototype design and Dingnan Rao's help in science writing.

**Conflicts of Interest:** The authors declare no conflict of interest.

## References

1. Alle, N.; Hiremath, S.S.; Makaram, S.; Subramaniam, K.; Talukdar, A. Review on electro hydrostatic actuator for flight control. *Int. J. Fluid Power* **2016**, *17*, 125–145. [[CrossRef](#)]
2. Kumar, M. A survey on electro hydrostatic actuator: Architecture and way ahead. *Mater. Today Proc.* **2021**, *45*, 6057–6063. [[CrossRef](#)]
3. Maré, J.-C.; Fu, J. Review on signal-by-wire and power-by-wire actuation for more electric aircraft. *Chin. J. Aeronaut.* **2017**, *30*, 857–870. [[CrossRef](#)]
4. Sun, W.; Wang, X.; Zhang, C. A Model-Free Control Strategy for Vehicle Lateral Stability with Adaptive Dynamic Programming. *IEEE Trans. Ind. Electron.* **2020**, *67*, 10693–10701. [[CrossRef](#)]
5. Sivčev, S.; Coleman, J.; Omerdić, E.; Dooly, G.; Toal, D. Underwater manipulators: A review. *Ocean. Eng.* **2018**, *163*, 431–450. [[CrossRef](#)]
6. Fu, Y.; Han, X.; Sepehri, N.; Zhou, G.; Fu, J.; Yu, L.; Yang, R. Design and performance analysis of position-based impedance control for an electrohydrostatic actuation system. *Chin. J. Aeronaut.* **2018**, *31*, 584–596. [[CrossRef](#)]
7. Law, M.; Wabner, M.; Colditz, A.; Kolouch, M.; Noack, S.; Ihlenfeldt, S. Active vibration isolation of machine tools using an electro-hydraulic actuator. *CIRP J. Manuf. Sci. Technol.* **2015**, *10*, 36–48. [[CrossRef](#)]
8. Navatha, A.; Bellad, K.; Hiremath, S.S.; Karunanidhi, S. Dynamic Analysis of Electro Hydrostatic Actuation System. *Procedia Technol.* **2016**, *25*, 1289–1296. [[CrossRef](#)]
9. Belloli, D.; Previdi, F.; Savaresi, S.M.; Cologni, A.; Zappella, M. Modeling and Identification of an Electro-Hydrostatic Actuator. *IFAC Proc. Vol.* **2010**, *43*, 620–625. [[CrossRef](#)]
10. Guo, Q.; Zhang, Y.; Celler, B.G.; Su, S.W. State-Constrained Control of Single-Rod Electrohydraulic Actuator with Parametric Uncertainty and Load Disturbance. *IEEE Trans. Contr. Syst. Technol.* **2018**, *26*, 2242–2249. [[CrossRef](#)]
11. Li, S.; Du, X.; Zhang, L.; Chen, K.; Wang, S. Study on dynamic characteristics of underwater pressure compensator considering nonlinearity. *Mech. Sci.* **2020**, *11*, 183–192. [[CrossRef](#)]
12. Wu, J.-B.; Li, L.; Wei, W. Research on dynamic characteristics of pressure compensator for deep-sea hydraulic system. *Proc. Inst. Mech. Eng. Part M J. Eng. Marit. Environ.* **2021**, *236*, 19–33. [[CrossRef](#)]
13. Guo, Q.; Zhang, Y.; Celler, B.G.; Su, S.W. Backstepping Control of Electro-Hydraulic System Based on Extended-State-Observer With Plant Dynamics Largely Unknown. *IEEE Trans. Ind. Electron.* **2016**, *63*, 6909–6920. [[CrossRef](#)]
14. Sun, W.; Pan, H.; Gao, H. Filter-Based Adaptive Vibration Control for Active Vehicle Suspensions with Electrohydraulic Actuators. *IEEE Trans. Veh. Technol.* **2016**, *65*, 4619–4626. [[CrossRef](#)]
15. Mohanty, A.; Yao, B. Integrated Direct/Indirect Adaptive Robust Control of Hydraulic Manipulators with Valve Deadband. *IEEE/ASME Trans. Mechatron.* **2011**, *16*, 707–715. [[CrossRef](#)]
16. Yao, B.; Bu, F.; Reedy, J.; Chiu, G.-C. Adaptive robust motion control of single-rod hydraulic actuators: Theory and experiments. *IEEE/ASME Trans. Mechatron.* **2000**, *5*, 79–91. [[CrossRef](#)]

17. Lyu, L.; Chen, Z.; Yao, B. Advanced Valves and Pump Coordinated Hydraulic Control Design to Simultaneously Achieve High Accuracy and High Efficiency. *IEEE Trans. Contr. Syst. Technol.* **2021**, *29*, 236–248. [[CrossRef](#)]
18. Temporelli, R.; Boisvert, M.; Micheau, P. Control of an Electromechanical Clutch Actuator Using a Dual Sliding Mode Controller: Theory and Experimental Investigations. *IEEE/ASME Trans. Mechatron.* **2019**, *24*, 1674–1685. [[CrossRef](#)]
19. Shen, W.; Wang, J. An integral terminal sliding mode control scheme for speed control system using a double-variable hydraulic transformer. *ISA Trans.* **2019**, S0019-0578(19)30414-8. [[CrossRef](#)]
20. Kim, M.J.; Chung, W.K. Disturbance-Observer-Based PD Control of Flexible Joint Robots for Asymptotic Convergence. *IEEE Trans. Robot.* **2015**, *31*, 1508–1516. [[CrossRef](#)]
21. Lee, W.; Kim, M.J.; Chung, W.K. Asymptotically Stable Disturbance Observer-Based Compliance Control of Electrohydrostatic Actuators. *IEEE/ASME Trans. Mechatron.* **2020**, *25*, 195–206. [[CrossRef](#)]
22. Ahn, K.K.; Nam, D.N.C.; Jin, M. Adaptive Backstepping Control of an Electrohydraulic Actuator. *IEEE/ASME Trans. Mechatron.* **2014**, *19*, 987–995. [[CrossRef](#)]
23. Yao, J.; Deng, W. Active disturbance rejection adaptive control of uncertain nonlinear systems: Theory and application. *Nonlinear Dyn.* **2017**, *89*, 1611–1624. [[CrossRef](#)]
24. Yao, J.; Jiao, Z.; Ma, D. Adaptive Robust Control of DC Motors with Extended State Observer. *IEEE Trans. Ind. Electron.* **2014**, *61*, 3630–3637. [[CrossRef](#)]
25. Luo, C.; Yao, J.; Gu, J. Extended-state-observer-based output feedback adaptive control of hydraulic system with continuous friction compensation. *J. Frankl. Inst.* **2019**, *356*, 8414–8437. [[CrossRef](#)]
26. Lin, T.; Lin, Y.; Ren, H.; Chen, H.; Li, Z.; Chen, Q. A double variable control load sensing system for electric hydraulic excavator. *Energy* **2021**, *223*, 119999. [[CrossRef](#)]
27. Lyu, L.; Chen, Z.; Yao, B. Development of Pump and Valves Combined Hydraulic System for Both High Tracking Precision and High Energy Efficiency. *IEEE Trans. Ind. Electron.* **2019**, *66*, 7189–7198. [[CrossRef](#)]
28. Cheng, M.; Zhang, J.; Xu, B.; Ding, R.; Wei, J. Decoupling Compensation for Damping Improvement of the Electrohydraulic Control System with Multiple Actuators. *IEEE/ASME Trans. Mechatron.* **2018**, *23*, 1383–1392. [[CrossRef](#)]
29. Ding, R.; Cheng, M.; Jiang, L.; Hu, G. Active Fault-Tolerant Control for Electro-Hydraulic Systems with an Independent Metering Valve Against Valve Faults. *IEEE Trans. Ind. Electron.* **2021**, *68*, 7221–7232. [[CrossRef](#)]
30. Kim, M.J.; Beck, F.; Ott, C.; Albu-Schaffer, A. Model-Free Friction Observers for Flexible Joint Robots with Torque Measurements. *IEEE Trans. Robot.* **2019**, *35*, 1508–1515. [[CrossRef](#)]
31. Helian, B.; Chen, Z.; Yao, B.; Lyu, L.; Li, C. Accurate Motion Control of a Direct-Drive Hydraulic System with an Adaptive Nonlinear Pump Flow Compensation. *IEEE/ASME Trans. Mechatron.* **2021**, *26*, 2593–2603. [[CrossRef](#)]
32. Helian, B.; Chen, Z.; Yao, B. Precision Motion Control of a Servomotor-Pump Direct-Drive Electrohydraulic System with a Nonlinear Pump Flow Mapping. *IEEE Trans. Ind. Electron.* **2020**, *67*, 8638–8648. [[CrossRef](#)]
33. Ren, G.; Esfandiari, M.; Song, J.; Sepehri, N. Position Control of an Electrohydrostatic Actuator with Tolerance to Internal Leakage. *IEEE Trans. Contr. Syst. Technol.* **2016**, *24*, 2224–2232. [[CrossRef](#)]
34. Cai, Y. Research on Robust Control of Electro-Hydrostatic Actuators and Secondary Controlled Systems Based on Quantitative Feedback Theory. Ph.D. Thesis, Northeastern University, Shenyang, China, 2017. (In Chinese).
35. Han, J. From PID to Active Disturbance Rejection Control. *IEEE Trans. Ind. Electron.* **2009**, *56*, 900–906. [[CrossRef](#)]